THE ASTROPHYSICAL JOURNAL, 461:386–395, 1996 April 10

THE WOLF-RAYET STAR HD 197406 WITH ITS STRONGLY IONIZING CLOSE COMPANION

SERGEY V. MARCHENKO,[1,2] ANTHONY F. J. MOFFAT,[1] ROBERT LAMONTAGNE,[1] AND GAGHIK H. TOVMASSIAN[3]

Received 1995 August 4; accepted 1995 October 12

ABSTRACT

High-quality, phase-dependent CCD spectra are presented for the first time for this unusual Population I, runaway WN7 single-line binary system. Besides confirming a previous orbit based on the N IV 4058 Å emission line, these spectroscopic data show phase-dependent, line-profile variations, especially in He II. The low mass function, but normal orbital inclination, implies that the companion is either a normal B2–B4 V–III star or a relativistic object. In either case, the phase-dependent line variations lead to the suggestion of an ionized cavity near the companion that is probably created from X-rays generated via impact of the W-R wind on the windless B star, or via accretion on the relativistic companion. This is borne out in the light curve, based on new data combined with all previously published data, which shows a *broad* minimum when the W-R component is closest to the observer. Compared to all other light curves known for W-R + OB systems, HD 197406's light curve requires the secondary light to arise in an *extended* region, presumably the hot cavity. Some preference is shown for the scenario involving a relativistic companion, from timing arguments of the orbiting ionized cavity. Despite the strong ionization, its *local* nature ensures that HD 197406 remains only a weak observed X-ray source.

Subject headings: binaries: spectroscopic — stars: individual (HD 197406) — stars: Wolf-Rayet

1. INTRODUCTION

Before the infrared discovery that Cygnus X-3 likely contains a W-R star (van Kerkwijk et al. 1992), the single-line spectroscopic Wolf-Rayet (W-R) binary HD 197406 (WR 148) was considered among the most favorable candidate W-R + c (compact companion: a neutron star or a black hole) systems (Moffat 1983; Cherepashchuk & Aslanov 1984) mainly for two reasons: (*a*) runaway status from the possible recoil after a supernova explosion, leading to large separation from the Galactic plane, $z \sim 500$–800 pc (Moffat & Isserstedt 1980; Drissen et al. 1986; Dubner, Niemela, & Purton 1990), far exceeding the mean $z \sim 60$ pc for massive Population I W-R stars (van der Hucht et al. 1988); and (*b*) very low mass function, $f(m) = 0.28 \pm 0.06\ M_{\odot}$ (Drissen et al. 1986), compared to massive WR + OB binaries, which typically have $f(m) \gtrsim 2\ M_{\odot}$. W-R + c systems are important because they were the only heretofore missing link in the chain of evolution for massive binaries: O + O → c + W-R → c + c. However, a serious drawback of the compact-companion hypothesis for HD 197406 is that the calculated (cf. Stevens & Willis 1988) X-ray flux exceeds the observed flux, $6.04 \pm 3.14 \times 10^{32}$ ergs s^{-1} (Pollock, Haberl, & Corcoran 1995), by a factor of 10^2–10^3. Furthermore, the observations of Dubner et al. (1990) place a limit on the radio continuum emissivity that is much too low for a magnetized neutron star remaining after a supernova explosion. Hence, the evolutionary status of the HD 197406 binary remains uncertain.

Here we report on new spectroscopic and photometric observations of HD 197406. They reveal indirect evidence for strong ionizing flux generated by the interaction of the W-R wind with the companion, which must be either a faint, low-mass, mid-B type, luminosity class V–III star, or a compact companion.

2. OBSERVATIONS

2.1. *Spectroscopy*

All the spectra were collected in 1988–1989 (eight spectra) and 1994 (14 spectra) using the 1.6 m telescope of the Mont Mégantic Observatory equipped with a Boller & Chivens spectrograph at the Cassegrain focus. In 1988–1989, an RCA 578 × 320 pixel CCD was used, providing a resolution of $\Delta\lambda = 2.9$ Å (2.2 pixels) in the wavelength range 3550–4300 Å and S/N ~ 100–150 per pixel in the continuum for a 1.5–2.0 hr exposure. In 1994, the spectra were taken with a Thompson 1024 × 1024 pixel CCD, $\Delta\lambda = 2.4$ Å (2.9 pixels) in the range 3720–4560 Å and S/N ~ 200–250 with typical exposures of 2.0–2.7 hr. Standard reduction procedures (bias subtraction, flat-field and dispersion curve correction, etc.) were performed using IRAF. As a rule, the radial velocities (RVs) refer to the centroid of the emission line. The data are presented in Table 1: column (1) gives the heliocentric Julian Date (HJD) of mid-exposure; column (2) the orbital phase in accordance with Drissen et al. (1986), column (3) the measured heliocentric radial velocity (RV) of the emission line N IV λ4058, and columns (4) and (5) the heliocentric RVs of the weak, ~central absorption components of He II + Hγ λ4340 and He I λ4471.

2.2. *Photometry*

In this paper we shall make use of both published (Bracker 1979; Antokhin 1984; Moffat & Shara 1986) and new photoelectric photometry from two runs. The first run was carried out at the Wise Observatory (Israel) in 1989 (see Lamontagne et al. 1995 for details). The second run was in 1994 June–July using a one-channel pulse-counting photometer attached to the 0.84 m telescope of the San

[1] Département de Physique, Université de Montréal, C.P. 6128, Succursale Centre-Ville, Montreal, Québec, H3C 3J7, Canada, and Observatoire du Mont Mégantic; sergey, moffat, lamont@astro.umontreal.ca.

[2] On leave from Main Astronomical Observatory of the Ukrainian Academy of Sciences, Goloseevo, 252127 Kiev, Ukraine.

[3] Instituto de Astronomía, Apartado Postal 877, C.P. 22860, Ensenada, Mexico; gag@bufadora.astrosen.unam.mx.

TABLE 1

SUMMARY OF THE MONT MÉGANTIC SPECTROSCOPIC OBSERVATIONS IN 1988–1994

HJD −2,440,000 (1)	PHASE[a] (2)	EMISSION RV(4057.80 Å) (km s^{-1}) (3)	ABSORPTION RV(4338.67 Å) (km s^{-1}) (4)	ABSORPTION RV(4471.48 Å) (km s^{-1}) (5)
7,347.706......	0.262	−36.6	...	...
7,491.653......	0.603	−211.5	...	...
7,492.622......	0.828	−215.9	...	...
7,745.745......	0.457	−110.7	...	...
7,749.819......	0.400	−92.4	...	...
7,755.705......	0.764	−193.1	...	...
7,757.707......	0.228	−37.2	...	...
7,763.782......	0.635	−209.3	...	...
9,558.683......	0.374	−75.9	−127.5	−153.9
9,616.687......	0.810	−198.2	...	...
9,616.796......	0.835	−230.1	...	...
9,637.558......	0.644	−210.0	...	...
9,637.654......	0.666	−223.3	...	...
9,638.526......	0.868	−164.4	...	...
9,638.630......	0.892	−169.7	...	−157.9
9,639.539......	0.103	−38.5	...	...
9,640.543......	0.335	−80.2	−167.7	−167.9
9,640.653......	0.361	−78.2	−174.1	−168.8
9,641.523......	0.562	−212.2	...	−93.9
9,641.627......	0.586	−253.6	...	...
9,642.527......	0.795	−182.0	...	...
9,642.630......	0.819	−197.2	...	−118.5

[a] According to the ephemeris of Drissen et al. 1986 for phase zero (W-R star in front): JD 2,432,434.4 + 4^{d}.317364E.

Pedro Martir Observatory (Baja California, México). These observations were carried out in broadband V (Johnson) 2–3 times per night, following the cycle: sky–c2–c1–WR–c1–WR–c1–c2–sky, with 60 s integrations and c1, c2 comparison stars from a parallel program of long-term monitoring of northern WN8 stars. It was found to be relatively stable during the 4 week interval, with only slight night-to-night variations. We used the mean value $k_V = 0.277$ for the whole 1994 data set. The observations are listed in Table 2: column (1) gives the heliocentric mean JD of observation; columns (2) and (3) refer to V magnitudes for W-R − cl and c2 − c1, respectively. The overall σ(c2 − c1) accuracy is 0.006 mag in 1989 and 0.004 mag in 1994. It is obvious from our data and all previous observations that HD 197406 is very active on timescales ranging from some seconds (intrinsic flickering and flaring mainly in the He II + Hβ 4860 Å emission line; see Zhilyaev, Khalack, & Verlyuk 1995; Khalack & Zhilyaev 1995) to weeks, months, and years, with a significant stochastic component sometimes dominating over the regular phase variations (cf. Antokhin & Cherepashchuk 1989).

3. RESULTS AND DISCUSSION

3.1. *Orbital Elements*

In an attempt to improve the orbital elements, all 85 available measurements of the most reliable emission line, N IV λ4058, were combined into one data set (Wilson 1948; Bracher 1979; Moffat & Seggewiss 1980; Drissen et al. 1986). Despite the differences in technique of RV measurements, no data show any significant systematic deviations (Fig. 1). This is substantiated by the fair agreement of the mean RVs of the interstellar Ca II H and K lines, which are $-27.8 \pm 11(\sigma)$ km s^{-1} from the present work, −37.5 km s^{-1} (Wilson 1948), −51.1 km s^{-1} (Bracher 1979), and −40.0 km s^{-1} (Moffat & Seggewiss 1980). The N IV 4058 Å emission is a fairly narrow and symmetric line, not seriously affected by the presence of the companion (see below). There is no difference between its RV measured on the whole profile and its RV based on the upper half of the line.

Most measurable spectral features (in both absorption and emission; see the mean spectrum in Fig. 2) move in

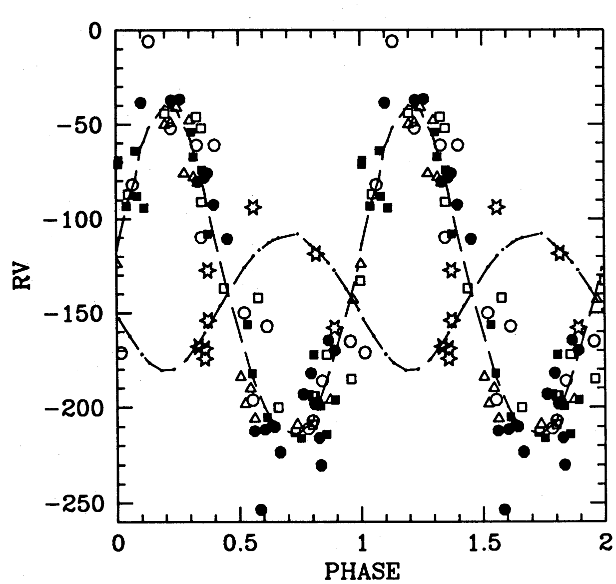

FIG. 1.—Radial velocity versus orbital phase (see Table 1) for the well-behaved W-R emission line N IV λ4058. Open squares denote the RV (in km s^{-1}) of Wilson (1948); filled squares correspond to Bracher (1979); open triangles are from Moffat & Seggewiss (1980); open circles give the RV of Drissen et al. (1986); filled circles and starred symbols refer to the present data (N IV 4058 Å emission and weak absorptions at He II + Hγ 4340 Å and He I 4471 Å, respectively). Curves are orbital fits from Table 3.

TABLE 2

NEW BROADBAND (V) PHOTOMETRY OF HD 197406 IN 1989 AND 1994

HJD 2,440,000 (1)	Phase (2)	W-R − c1 (3)	c2-c1 (4)	HJD 2,440,000 (1)	Phase (2)	W-R − c1 (3)	c2-c1 (4)
7,680.560......	0.358	0.067	0.081	7,701.498......	0.208	0.119	0.091
7,684.548......	0.282	0.070	0.082	7,702.519......	0.445	0.092	0.092
7,685.489......	0.500	0.091	0.089	7,703.424......	0.654	0.094	0.093
7,689.417......	0.410	0.075	0.093	7,704.425......	0.886	0.130	0.097
7,690.417......	0.642	0.091	0.087	7,704.478......	0.898	0.131	0.098
7,691.437......	0.878	0.122	0.095	7,704.549......	0.915	0.130	0.100
7,692.429......	0.108	0.109	0.097	7,705.376......	0.106	0.119	0.088
7,692.442......	0.111	0.101	0.078	7,705.474......	0.129	0.122	0.096
7,693.419......	0.337	0.093	0.098	7,705.544......	0.145	0.118	0.095
7,965.418......	0.800	0.106	0.096	7,706.405......	0.345	0.095	0.096
7,696.440......	0.037	0.118	0.095	7,706.548......	0.378	0.094	0.098
7,697.434......	0.267	0.096	0.085	7,707.428......	0.582	0.093	0.094
7,698.433......	0.498	0.083	0.094	7,707.528......	0.605	0.096	0.092
7,699.430......	0.729	0.099	0.094	7,708.396......	0.806	0.112	0.083
7,700.470......	0.970	0.112	0.097	7,708.557......	0.843	0.109	0.094
9,520.782......	0.596	0.084	...	9,534.728......	0.826	0.104	0.092
9,521.742......	0.818	0.090	0.092	9,535.686......	0.048	0.105	0.089
9,521.825......	0.838	0.097	0.092	9,536.720......	0.288	0.100	0.094
9,522.747......	0.051	0.082	0.091	9,536.812......	0.309	0.104	0.094
9,522.858......	0.077	0.089	0.088	9,536.897......	0.328	0.101	0.085
9,522.945......	0.097	0.088	0.088	9,537.745......	0.525	0.075	0.084
9,523.878......	0.313	0.096	0.089	9,537.850......	0.549	0.080	0.093
9,524.792......	0.525	0.096	0.089	9,537.921......	0.566	0.077	0.090
9,724.905......	0.551	0.088	0.096	9,538.716......	0.750	0.132	0.085
9,524.962......	0.564	0.101	0.086	9,538.822......	0.774	0.111	0.094
9,525.731......	0.742	0.092	0.092	9,538.924......	0.798	0.113	0.093
9,525.821......	0.763	0.099	0.084	9,539.749......	0.989	0.142	0.085
9,525.906......	0.783	0.107	0.093	9,539.865......	0.016	0.134	0.081
9,525.940......	0.791	0.102	0.093	9,540.818......	0.237	0.103	0.087
9,525.951......	0.793	0.108	0.096	9,540.909......	0.258	0.096	0.089
9,526.710......	0.969	0.090	0.087	9,540.979......	0.274	0.094	0.088
9,526.839......	0.999	0.107	0.095	9,541.728......	0.448	0.092	0.086
9,526.939......	0.022	0.106	0.089	9,541.826......	0.470	0.102	0.096
9,527.771......	0.215	0.098	0.094	9,541.921......	0.492	0.095	0.095
9,528.843......	0.463	0.078	0.093	9,542.759......	0.686	0.092	0.090
9,529.816......	0.688	0.097	0.092	9,542.868......	0.712	0.085	0.097
9,530.808......	0.918	0.121	0.091	9,543.732......	0.912	0.102	0.087
9,531.788......	0.145	0.116	0.090	9,543.832......	0.935	0.105	0.091
9,533.732......	0.595	0.122	0.094	9,543.954......	0.963	0.113	0.094
9,553.915......	0.638	0.105	0.099	9,544.816......	0.162	0.115	0.094
9,533.961......	0.648	0.101	0.090				

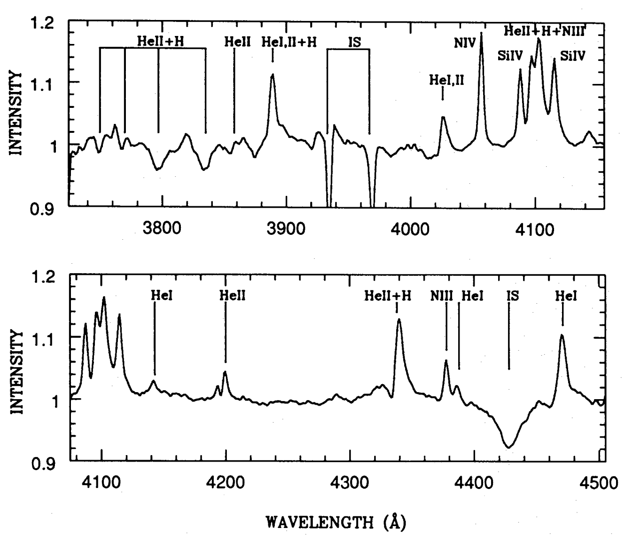

FIG. 2.—Mean rectified spectrum of HD 197406 based on the 1994 spectra listed in Table 1, after shifting each spectrum to the RV frame of reference defined by the N IV λ4058 orbit.

phase with the N IV line. Only the weak, ~central absorption features seen on top of He II + Hγ 4340 Å and He II 4471 Å at $\phi \sim 0.25$–0.40 and $\phi \sim 0.75$–0.80 (Fig. 3) appear to be moving in antiphase with the N IV line. However, one cannot seriously rely on their RV measurements: a formal test of their phase variability is statistically rejected by Fisher's criterion even at the 90% level. Nevertheless, we formally apply the Bertiau & Grobben (1969) algorithm simultaneously to the 85 RV measurements of the N IV line and the nine RV measurements of the 4340, 4471 Å absorption, to derive the orbital elements listed in Table 3. All elements for the W-R component are in good agreement with previous determinations. Solving the RV orbits for N IV and the weak λ4340/λ4471 absorptions *independently*, we obtain practically the same elements for the W-R star, but different values for the companion, $K = 106 \pm 114$ km s^{-1} and $e = 0.23 \pm 0.43$, implying that the absorptions are compatible with constant RV. Their apparent visible antiphase motion from one side to the other of the emission peak could then be caused by the reflex shift of the underlying emission profile. In order to enhance the spectrum of

TABLE 3

New Orbital Elements for HD 197406[a]

Object	γ_0 (km s^{-1})	K (km s^{-1})	T_0 (−2,440,000)	ω	e	$a \sin i$ ($R_\odot$)
W-R star......	−133.4 ± 1.7	87.7 ± 2.4	9,639.961 ± 0.219	−1°0 ± 18°0	0.079 ± 0.030	7.5 ± 0.2
B star(?)	−142.2 ± 5.3	36.2 ± 9.4	...	...	...	3.1 ± 0.8

Note.—γ_0 = systemic velocity, K = RV amplitude, T_0 = HJD time of periastron passage, ω = angle between ascending node and periastron, e = eccentricity, and $a \sin i$ = semimajor orbital axis.

[a] Based on N IV λ4058 for the W-R component and He, H absorption lines for the companion.

the companion, all spectra were shifted to the RV frame of the companion and co-added (cf. Marchenko et al. 1995). To do this, the unknown RV amplitude was varied from 0 to 500 km s^{-1}. No enhanced details of a companion were detected for $K < 0$–250 km s^{-1}; for $K \geq 250$ km s^{-1}, the results are unreliable because of interference from the narrow underlying emissions and the sparseness of the adjusted spectra in phase space.

3.2. *Light-Curve Simulations*

In Figure 4, we plot the light curve based on all available photometric V data (see § 2.2 above), both direct (Fig. 4*a*) and binned (Fig. 4*b*). Compared to other W-R binaries with

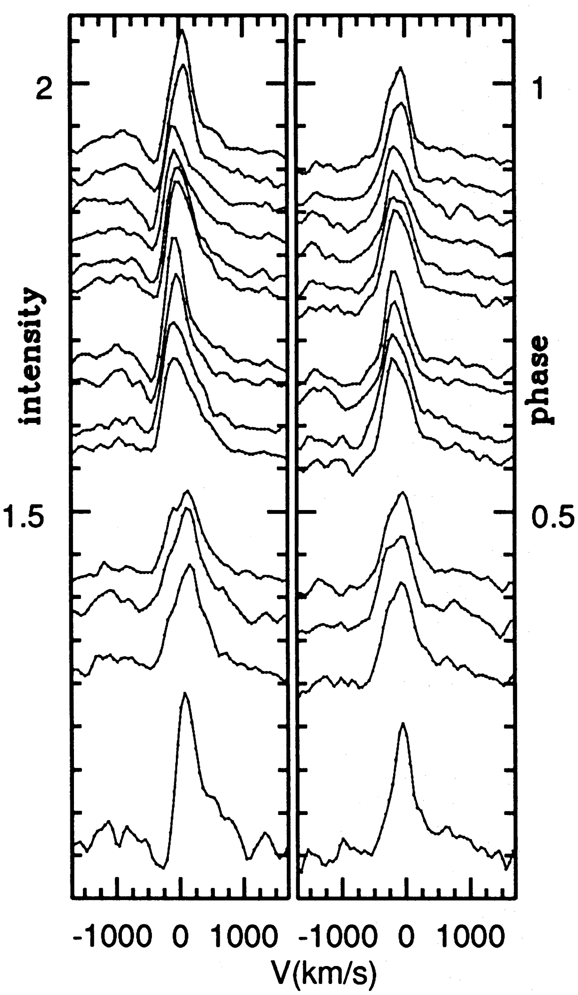

Fig. 3.—Montage of the 1994 spectra (Table 1) in velocity space for the He II + Hγ 4340 Å (*left*) and He I 4471 Å (*right*) lines. The rectified spectra are phased vertically in (approximate) proportion to the phase, indicated at right for the continuum level. The left ordinate scale is intensity in continuum units.

O companions, the light curve for HD 197406 is very noisy. Nevertheless, the lower noise binned light curve shows a rather flat, rounded minimum centered at $\phi = 0.0$ (W-R in front) with amplitude $\Delta V \sim 0.03$ mag. The shapes of light curves of known *non*core-eclipsing[4] W-R + O systems (due to phase-dependent attenuation of O star light; see Lamontagne et al. 1995) are, however, quite different: a V-shaped curve is always seen with minimum narrower than maximum.

One potential cause of the different light curve for HD 197406 may be that we are seeing the effects of electron scattering into the beam from free electrons in the W-R wind. If this were so, we would then expect such scattered light to follow the same behavior as the phase-dependent linear polarization found by Drissen et al. (1986). For simplicity, we assume the free electrons are distributed with spherical symmetry around the W-R component, as was done by St-Louis et al. (1988) to derive $\dot{M}$'s for W-R stars in binaries from polarimetric modulation. In the context of the polarization model of Brown et al. (1978), we would have an amplitude of the semimajor axis of the (normalized) polarization ellipse in the Q-U plane of

$$A_p = \tau_0 \gamma_3 (1 + \cos^2 i) ,$$

where τ_0 is an electron scattering optical depth, γ_3 is the distribution moment of the free electrons, and i is the orbital inclination. The full amplitude of the light variations *due to the same process* would be

$$\Delta I = 2 I_0 \tau_0 (\sin^2 i) \gamma_3 ,$$

where I_0 is the total unperturbed light. For small changes ΔI, we find a full *predicted* amplitude

$$\delta m_{\rm pred}({\rm mag}) = -2.5 \log [(I_0 - \Delta I)/I_0]$$
$$\simeq (5 \log e)[\sin^2 i/(1 + \cos^2 i)] A_p .$$

Thus, with observed values for HD 197406 (Drissen et al. 1986), $A_p = 0.0024$ and $i = 67°$, we get

$$\delta m_{\rm pred} = 0.0038 \text{ mag} ,$$

compared to the *observed* value, which is ~8 times larger. Despite the simplifications of this model, the differential nature of the above comparison suggests that light scattering by electrons *into* the line of sight is *not* the correct explanation for the light curve.

More likely, we are seeing scattering of light *out of the line of sight* by free electrons directly between the observer and the companion source that is orbiting in the W-R wind. Neglecting core eclipses (which are rare in any case), such a

[4] Note that all *core*-eclipsing WR + O systems with small-eccentricity orbits have two light-curve minima per orbit. This is definitely not the case for HD 197406.

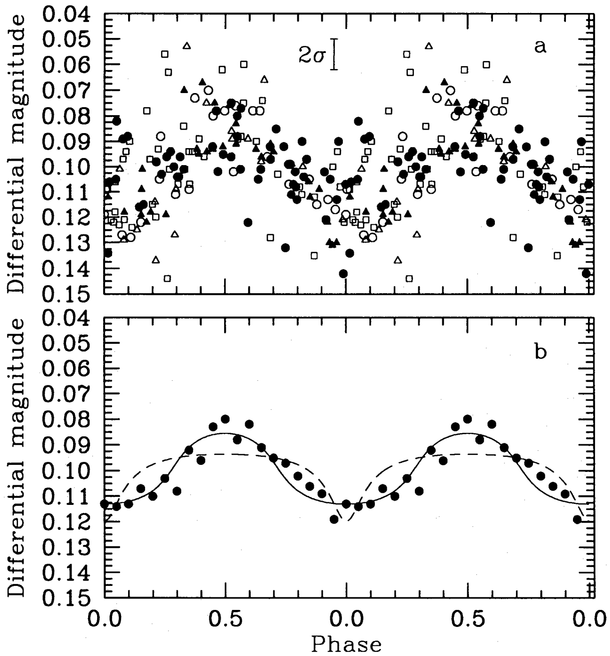

FIG. 4.—(*a*) Phase plot of individual data points of differential *V* magnitudes (*open triangles* are from Bracher 1979; *open squares*: Antokhin 1984; *open circles*: Moffat & Shara 1986; *filled triangles*: new 1989 data; *filled circles*: new 1994 data). The 2 σ error bar is a typical value based on the comparison star differences. (*b*) Same as (*a*), except that for clearer presentation the data are binned into 0.05 phase intervals. The full curve is a model fit to the *individual* data points of an azimuthally extended source (see text), while the dashed line is the V-shaped curve expected for a simple pointlike source orbiting with the same parameters in the wind.

scenario leads to a relatively-sharp V-shaped light-curve minimum (which degenerates into a sine wave only as $i \rightarrow 0$) centered at phase zero, when the W-R star is in front. Photometric observations of several W-R + O systems show this simple model to be quite valid in general (Lamontagne et al. 1995). However, in the case of WR 148, the light curve in Figure 4 (clearer in Fig. 4*b*) does not show this sharp V-shaped minimum. The rounded minimum is even broader than the maximum, which is anomalous for a simple point-source–like companion.

We construct a very simple but viable model to account for the light curve of WR 148. We begin with the simple model of a constant-velocity wind [$\beta = 0$; higher values of β, i.e., slower accelerations, do not change the shape significantly (see Lamontagne et al. 1995)] with an embedded pointlike source (a rather good approximation to an OB star disk with limb darkening, as it turns out):

$$\delta m = \delta m_0 + A(\pi/2 + \arcsin \epsilon)/(1 - \epsilon^2)^{1/2} , \qquad (1)$$

where δm_0 is a zero-point constant; $A = [(2.5 \log e)\alpha\sigma_e \dot{M}_{WR}]/[4\pi(1 + I_{WR}/I_O)m_p v_\infty a]$, a constant in which α is the number of free electrons per baryon mass m_p; σ_e is the Thompson single electron scattering cross section; $\dot{M}_{WR}$ is the mass-loss rate of the W-R component; I_{WR}/I_O is the light ratio of the W-R and companion stars,[5] v_∞ is the terminal velocity of the W-R wind; a is the mean orbital separation; and $\epsilon = (\sin i) \cos 2\pi\phi$, the only time-dependent variable.

Now we smear out the light curve (as observed, compared to a sharper V-shape) by introducing an extended source. In the simplest way, this can be done by extending the companion light source in the radial or the azimuthal direction, or both, relative to the W-R star. However, radial extension does not change the *shape* of the light curve, just its amplitude, and even then only by a small amount for a small symmetric extension about the mean separation. Therefore, we adopt a simple model of a uniform source with *total* emission intensity I_O at distance a from the center of the W-R star, that is, symmetrically extended along the orbit of the companion by an angle $\delta\phi$ in each direction. The light curve is then simulated by integrating equation (1) above, over phases $\phi \pm \delta\phi$, for each position of the companion in the orbit.

A fit to the light curve is then made with free parameters δm_0, A, and $\delta\phi$ (we fix $i = 66\overset{\circ}{.}7$, i.e., the value from polarization modulation; decreasing i does slightly improve the fit, consistent with HD 197406 being a non–core-eclipser, but there is no justification for this in the context of such a crude model). The final fit (Fig. 4*b*) yields $\delta m_0 = 0.069$, $A = 0.014$, and $\delta\phi = 103\overset{\circ}{.}5$. Taking $\alpha = \frac{1}{4}$ for He^+, which must dominate the scattering part of the wind along the line of sight in this cool WN stars; and taking $I_{WR}/I_O = 5$ (from the observed degree of phase-dependent change in ionization of the He I/He II lines); $v_\infty = 1250$ km s^{-1} (mean of values of Schmutz, Hamann, & Wessolowski 1989; and Rochowicz & Niedzielski 1995), and $\dot{M}_{WR} = 5 \times 10^{-5}$ $M_\odot$ yr^{-1}, typical for WNL stars (Leitherer, Chapman, & Koribalski 1995), lead to $a = 38$ $R_\odot$ for $i = 66\overset{\circ}{.}7$. This is compatible with estimates of the orbital dimension from the observed mass function for the WNL component combined with $i = 66\overset{\circ}{.}7$ and companion mass 5–10 $M_\odot$ for a B2–B4 V–III star or BH: $a = 29$–41 $R_\odot$, respectively. It is interesting to note that the total arc length $2\delta\phi = 207°$ corresponds well with the orbital phase interval 0.25–0.9 [(0.9–0.25) × 360° = 234°], in which the ionized source is in front of the W-R star (see below). This simple model will be incorporated later with the spectral variations to construct a cartoon model of the system.

3.3. *Origin of the "Central" Absorptions at 4340 and 4471* Å

The question of the origin of the weak absorptions on the tops of the emission lines He II + Hγ 4340 and He I λ4471 has utmost importance in clarifying the nature of the companion. Below, we discuss several possibilities.

a) As a first and most obvious possibility, the absorptions could arise in a companion star of early B type and modest (V–III) luminosity class. Attributing the central absorption at 4340 Å to Hγ, these weak absorptions have comparable equivalent widths of $\sim$0.01 Å, implying spectral class B2–B4 and luminosity ratio $L_{WR}/L_{comp} \gtrsim 50$. This ratio roughly satisfies the assumption of both a B2–B4 V–III spectrum for the companion (cf. empirical Hγ-luminosity calibration of Millward & Walker 1985) and of a lower limit to the total brightness of the system: $M_v = -5.4$ mag (Dubner, Niemela, & Purton 1990). Such a star would have a mass of $\sim$5–10 $M_\odot$, and thus an orbital velocity amplitude $K_{comp} \sim 230$–360 km s^{-1}. The *observed* radial velocity amplitude of the central absorptions ($K_{comp} = 36$ km s^{-1}) may be seriously underestimated because we are missing the key phases of maximum RV expected at $\phi \sim 0.25$ and

[5] Note that while the stellar luminosity ratio could be as much as 50 in the case of a main-sequence companion, the observed light ratio could be close to 3–5, since $\lesssim$50% of He II is ionized by the X-ray source, and we are observing the W-R light scattered by these additional electrons as the extended light source.

$\phi \sim 0.75$, due to unfavorable location of the absorptions (blended with the P Cygni absorption edge of the W-R star at $\phi \sim 0.2$ and moving toward the red edge of the W-R emission profile at $\phi \sim 0.7$). Clearly, observations with higher spectral resolution are needed to resolve the profiles of the absorptions and trace their *complete* orbital motion, if present.

b) A second possibility is that we are correctly estimating $K_{\rm comp} = 36$ km s^{-1} which, when combined with $K_{\rm WR} = 88$ km s^{-1}, makes the W-R star a low-mass ($\sim 0.3\ M_{\odot}$) Population II object, i.e., a planetary nebula (PN) with a W-R-type central star. This case meets some objections. Inspection of the W-R spectrum (Conti 1995; cf. also our Fig. 2) does not reveal any nebular emission lines. Furthermore, all known PNs with W-R–type central objects belong to the WC sequence (Tylenda, Acker, & Stenholm 1993), with only one exception: N66 in the LMC (Peña et al. 1995). Finally, all known PNs have $M_V \leq -2.2$ mag, while $M_v \geq -5.4$ mag for HD 197406. In particular, the adopted value $M_v = -5.4$ cannot be significantly decreased, because the lower limit of the distance to HD 197406 ($\sim$4.5 kpc) is determined by the negative velocities of the interstellar (IS) H and K Ca II lines ($V_{\rm HeI} = -30$–40 km s^{-1}).

c) Hence, the assumption that the W-R component is a normal Population I star seems to be quite plausible. In this case the companion is either a B2–B4 V–III star (as noted above) or a relativistic object. As noted previously, the phase modulation of the weak absorption RVs could be artificially introduced by motion of the underlying emission lines. If RV is constant, these absorptions could originate in an envelope expelled during a RLOF (Roche Lobe overflow) episode of the initially more massive star. However, a deep search for any nebulosity around HD 197406 in Hα+ [N II] lines yielded negative results (Miller & Chu 1993). This could indicate that the nebulosity has formed too recently to have reached 2″ in size (the spatial resolution of Miller & Chu). The origin of the weak absorptions in circumstellar gas is supported by the survey of Nichols & Fesen (1994), who found that HD 197406 is one of two W-R stars (the other one is HD 143414 = WR 71) exhibiting high-velocity interstellar components in their environments, but not known to lie inside an OB association or have an associated optical ring nebula. There are definite high-speed Mg II and Fe II IS components at -40 and -70 km s^{-1}, and possible components in Mg II at $+30$ and -120 km s^{-1}, the latter being coincident with the estimated systemic velocity $\gamma = -142 \pm 5$ km s^{-1} of the weak, central absorptions (Table 3). We note that, in the early phase of nova eruptions, the expelled matter can be seen as (e.g., Balmer) photospheric absorption lines (cf. Payne-Gaposhkin 1957).

d) A final possibility is that the absorptions are only apparent, being caused by lack of emission (i.e., "evaporated" W-R wind) or, alternatively, by additional emission arising around the companion, in intriguing resemblance to the high-mass X-ray binary HD 153919/4U 1700−37 (Blake et al. 1995). Indeed, there is a clear indication that the radiation field emerging from the companion has an effect on the profiles of the He I/He II lines (Fig. 5). However, the evaporated regions are located mainly at $v \leq -300$ km s^{-1} at $\phi \sim 0.5$, while the weak absorptions always have $v \geq -180$ km s^{-1} (see Fig. 1). If the weak absorptions are only apparent, as a result of an additional emission peak arising around the companion (cf. the numerical simulations of Koenigsberger 1995), it would be hard to explain why this emission peak suddenly jumps from $v \sim -250$ km s^{-1} at $\phi \sim 0.4$ to $v \sim 0$ km s^{-1} at $\phi \geq 0.55$ (see Fig. 3). Although of reduced amplitude, this variability also reminds one of the V/R variations seen in Be-type stars and in the optical lines of the W-R star HD 50896 (Smith & Willis 1994; St-Louis 1994), another suspected W-R + c binary or single rotating star with an inhomogeneous wind. It would be interesting to search for any wind-flattening effects in HD 197406 in this context. The *UBVRI* snapshot polarimetry for HD 197406 of Moffat et al. (1995) shows that, if there is any intrinsic polarization, it must be less than 0.4%. This weakens, but does not exclude, the possibility of a slightly flattened wind.

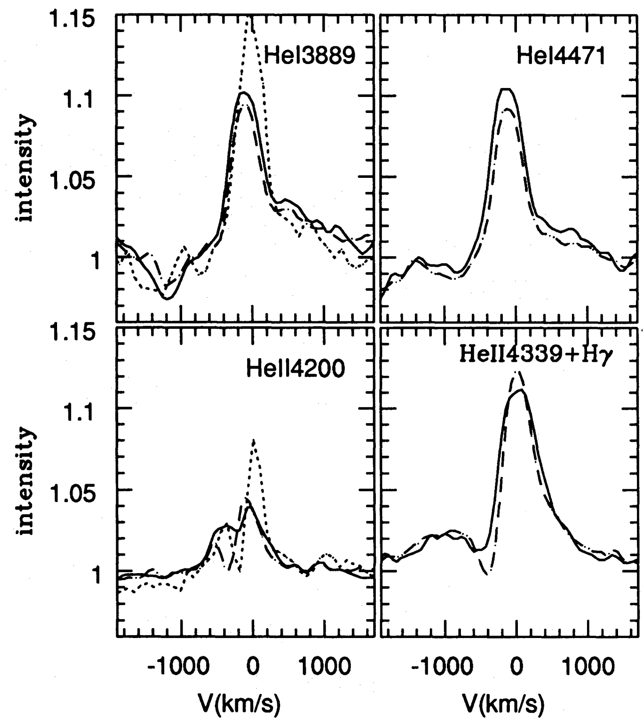

FIG. 5.—Mean (0.1 bins) profiles of four main emission lines in HD 197406 at phases 0.24 (*dotted line*), 0.50 (*full line*), and 0.85 (*dashed line*).

3.4. *Influence of the Companion on the W-R Wind Structure*

In Figures 6 and 7 we show gray-scale plots and equivalent widths of the major emission lines, supplementing our previous finding of strong phase dependence of the He I/He II profiles (Fig. 5). On the other hand, the N IV 4058 Å line varies little, maintaining its reliability as a good tracer of the W-R orbit. This line virtually escapes the influence of the ionizing flux (Fig. 7), because it is formed much closer to the W-R core than any of the He I/He II lines (e.g., the bulk of N IV emission is formed at $r \sim 3R_*$ in the case of the WN5 star HD 50896 [Hillier 1989]; in HD 197406, WN7, this line will be formed even closer). The common feature clearly seen in Figure 6 is that all He I/He II lines (some are blended with H) experience the influence of the companion's radiation field, in the sense that both the emission and absorption components of the P Cygni profiles are reduced at $\phi \sim 0.5^{+0.3}_{-0.2}$ (companion in front) compared to the "restored" W-R wind at $\phi = 0.90$–1.25. Surprisingly, the He I lines are affected less than the He II lines (cf. also Fig. 5), and He I λ3889 even reaches a secondary maximum at $\phi \sim 0.6$–0.7 (compared to primary maximum at $\phi \sim 0.1$–

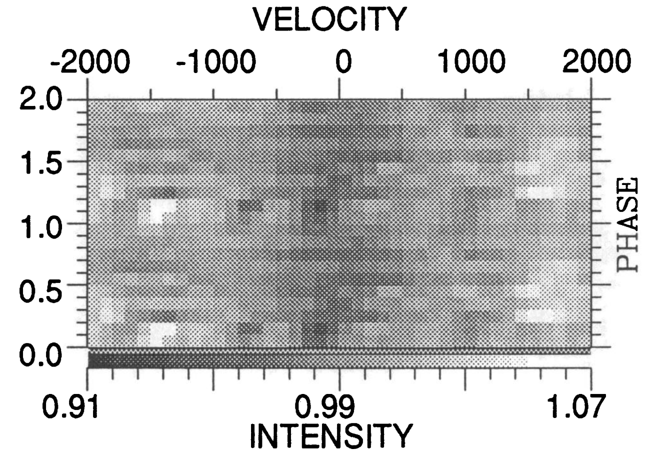

FIG. 6*a*

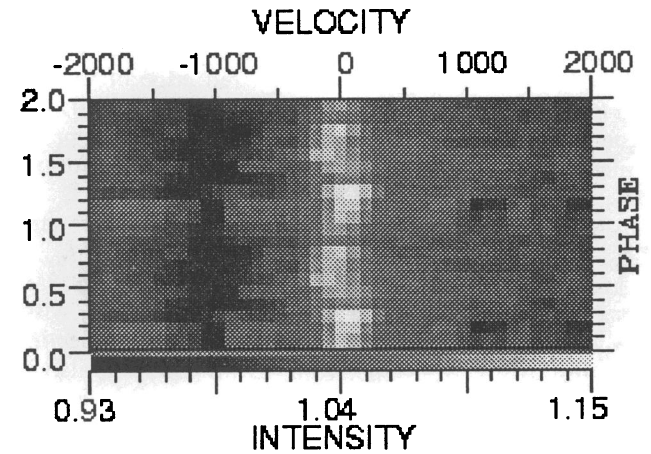

FIG. 6*b*

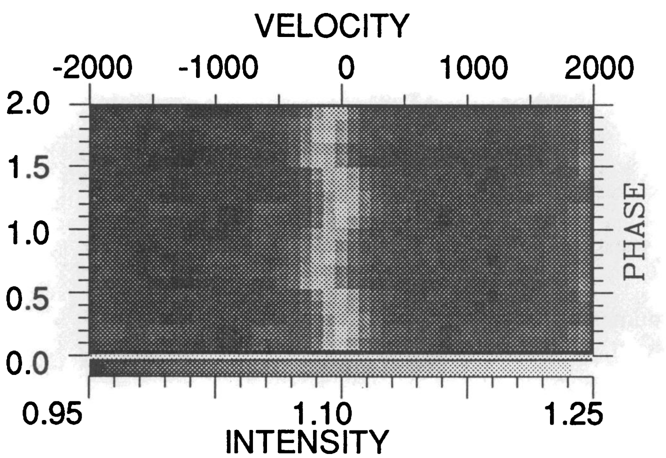

FIG. 6*c*

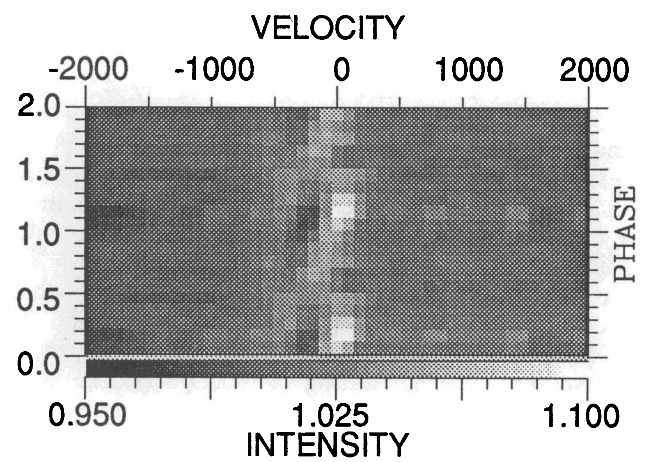

FIG. 6*d*

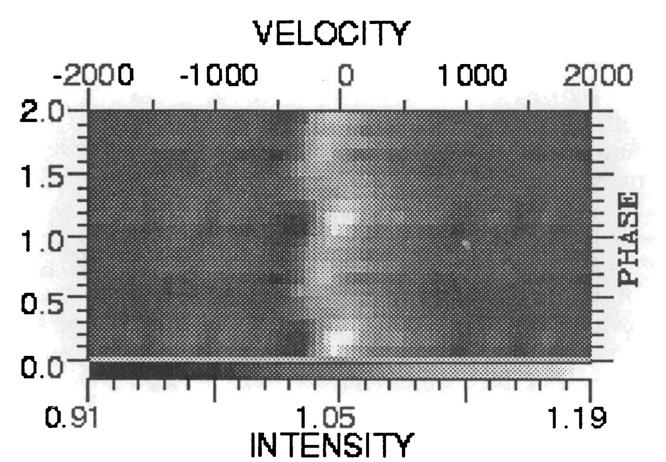

FIG. 6*e*

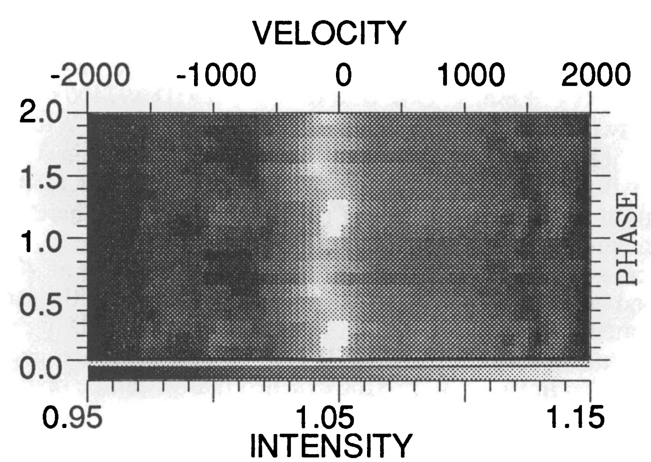

FIG. 6*f*

FIG. 6.—Gray-scale plots of the major lines from the rectified spectra: (*a*) He II + H9 3835 Å; (*b*) He I + H8 3889 Å (*c*) N IV 4058 Å; (*d*) He II 4200 Å; (*e*) He II + Hγ 4340 Å, and (*f*) He I 4471 Å. All available spectra are averaged within 0.1 phase bins (0.0–0.1, 0.1–0.2, etc.). When data are lacking, the corresponding spectrum is produced by linear interpolation between the subsequent bins.

0.2), when He II λ4200 is the most affected. The P Cygni absorption component of He I λ4471 is gradually restored starting from $\phi \sim 0.5$, i.e., $\Delta\phi = 0.1$–0.2 earlier than the P Cygni absorptions of He II + Hγ λ4340 and He II λ4200. All this means that the ionizing source around the companion is localized mainly in the zone of He II line formation, with little influence on the "distant" He I 3889 Å line and, even to a lesser extent, the "close" (cf. the W-R core) N IV 4058 Å line.

Two possibilities immediately emerge from this. First, the W-R wind could be crashing onto the surface of the B2–B4 V–III companion. This "crashing" scenario is supported by the fact that stellar winds suddenly turn on near B0–B1 V spectral class (Grigsby & Morrison 1995); thus, B2–B4 stars

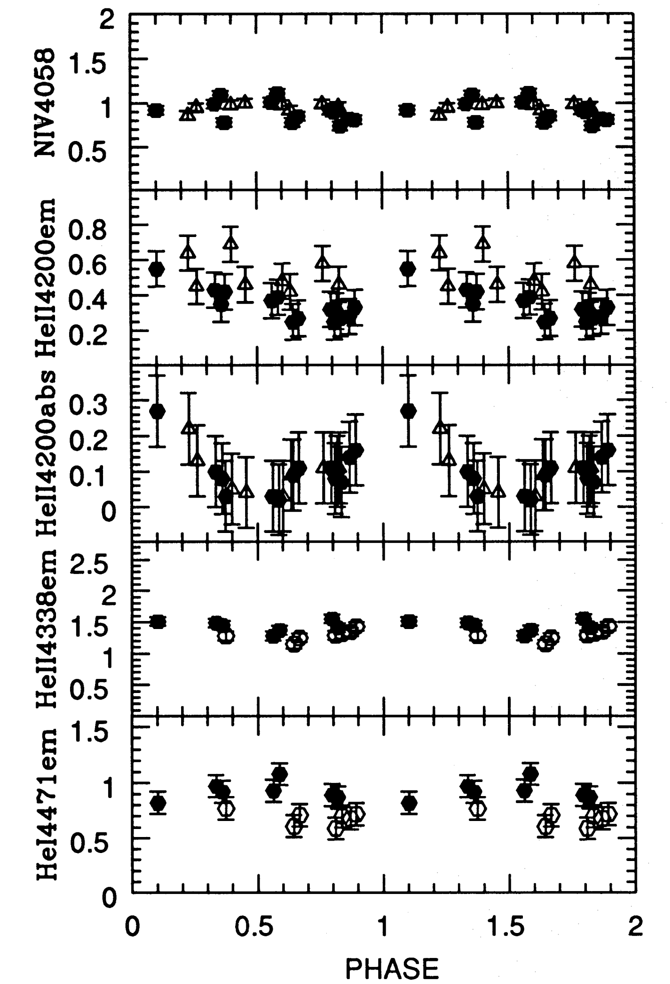

FIG. 7.—Equivalent width vs. phase of major lines. The emission values refer to the part of the line above the continuum, not allowing for the possible influence of absorption features. The absorption EW of He II 4200 refers to the area bound by a straight line between the two emission peaks and the observed profile. Open symbols for N IV 4058 and He II 4200 refer to the 1988–1989 data, and filled symbols refer to the 1994 data. Open symbols for He II 4338em and He I 4471em refer to the data taken between HJD 2449558 and HJD 2449638, and filled symbols refer to the data taken after HJD 2449638.

possess too weak a wind to prevent the crashing of the W-R wind onto their surfaces. The emerging X-ray flux can be evaluated from the energy conservation principle: $L_x = (A/2)\pi R_*^2 \rho_{\rm wind}(a)[v_{\rm wind}^2(a) + v_{\rm orb}^2]^{3/2}$, where A is the effectiveness of conversion of the wind kinetic energy into the X-ray radiation, typically ~ 0.1 (Shakura & Sunyaev 1973), $\rho_{\rm wind}$ and $v_{\rm wind}$ are the wind density and velocity at the orbital distance of the companion a, and R_* and $v_{\rm orb}$ are the radius and the orbital velocity of the companion. Taking $R_* = 6\ R_\odot$, $\rho_{\rm wind} \sim (0.5\text{–}1.6) \times 10^{-12}$ g cm^{-3} [for $\dot{M} = 5 \times 10^{-5}\ M_\odot$ yr^{-1}, $a = (29\text{–}41)\ R_\odot$, and $v_{\rm wind} = (4\text{–}6) \times 10^7$ cm s^{-1}], and $v_{\rm orb} \sim (2\text{–}3) \times 10^7$ cm s^{-1}, we obtain $L_x \sim 3 \times 10^{32}\text{–}10^{33}$ ergs s^{-1}. This X-ray flux is redirected mainly back toward the W-R star (see Fig. 8*a*), partially ionizing He II and only slightly affecting He I and N IV. In this case, one would expect the direction of maximum X-ray flux to be shifted toward the vector of the companion's orbital motion, i.e., causing maximum ionization to occur at $\phi \sim 0.3\text{–}0.4$. Note that the orbital velocity of the companion must be comparable to the W-R wind velocity (400–600 km s^{-1} at the orbital distance of the companion; cf. the evaporation of the P Cygni absorptions in Fig. 5). However, the He I 3889 and He II 4200 Å lines demonstrate the opposite effect, being more depressed at $\phi \sim 0.8$ than at $\phi \sim 0.25$ (Fig. 5).

An alternative model is the ionization caused by accretion of the wind onto a compact companion (Blondin 1994). This can naturally account for the phase asymmetry noted above, i.e., the fact that the maximum ionization occurs at $\phi \sim 0.7\text{–}0.8$ rather than at $\phi \sim 0.3\text{–}0.4$ (see Fig. 8*b*). In this model, the ionization of He I is altered at $0.5 \leq \phi \leq 0.7$ as a result of shadowing by the dense bow shock arm, and resumed at $\phi \sim 0.7\text{–}0.8$ because of the low absorption of X-ray flux inside the cavity in the W-R wind created by the orbiting companion.

Can we learn something about the nature of the companion from UV spectra? All available (low-resolution) spectra of HD 197406 were retrieved from the *IUE* archive: SWP 14131 ($\phi = 0.984$), SWP 14145 (0.223), SWP 14171 (0.683),

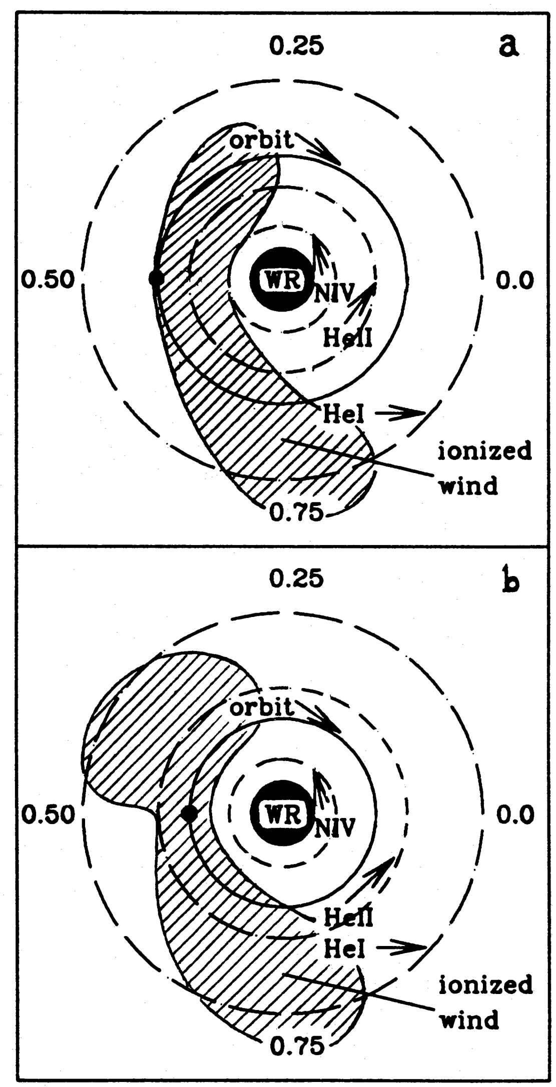

FIG. 8.—Cartoon model for a Population I WNL star with (*a*) an early B V–III companion and (*b*) a compact companion. The W-R star is shown fixed, while the companion orbits are shown with phases as indicated. Dashed circles indicate approximate ridges of maximum emission for N IV, He II, and He I lines. Hatched areas indicate the approximate extent of the W-R wind ionized by X-rays from (*a*) the W-R wind crashing onto the B star and (*b*) the accretion process onto the compact star.

SWP 14177 (0.750), SWP 14555 (0.819), SWP 14713 (0.474), SWP 15138 (0.287). Despite the sparse phase coverage, we confirm that the He II 1640 Å line reacts to the presence of the companion as do the optical He I/He II lines, exhibiting a minimum in intensity around $\phi \sim 0.2$–0.5 and being "restored" at $\phi \geq 0.9$. There is probably also a secondary minimum around $\phi = 0.8$. The slope of the UV continuum shows no phase dependency. Also, taking into account that as much as ~50% of He II can be ionized by the companion, we conclude that the peak of the companion's flux distribution is shifted below 228 Å (He II ionization limit). We note another important fact as indirect evidence for excess extreme-UV flux: the equivalent width of C IV 5806 Å emission in HD 197406 far exceeds the mean value for WN7–8 stars (Conti, Leep, & Perry 1983). Since this line can be formed via continuum fluorescence ($\lambda \leq 312$ Å continuum in the case of C IV 5806 Å; Hillier 1989), this easily leads to a UV (soft X-ray?) excess in HD 197406.

As noted above, if the companion is a normal star, it must be of type B2–B4 V–III with $M_{\rm comp} \sim 5$–$10\ M_\odot$ (for class V; see Andersen 1991). This brings the total mass of the system to $M \sim 17$–$53\ M_\odot$, if the inclination of the system $i = 63°$–$71°$ (Drissen et al. 1986). The system is thus peculiar among the Galactic W-R Population I stars both by virtue of its mass ratio, $M_{\rm comp}/M_{\rm WR} \approx 0.3 \pm 0.1$, and its distance from the Galactic plane, exceeding 500 pc.

If reliable, the significant negative radial velocity could strengthen the hypothesis of a W-R + c binary system running away from the Galactic plane after a supernova explosion; the *total* spatial velocity of HD 197406 would be $V \geq 150$ km s^{-1}, which is still possible as a limiting case for a symmetric supernova explosion in a very close binary (Moffat & Seggewiss 1979). How well does the γ-velocity derived from the N IV 4058 Å line reflect a true systemic velocity? The velocities of nitrogen lines tend to be more negative than the systemic velocities derived from independent assumptions (Underhill & Yang 1991; Smith & Willis 1994, and discussion therein). This can be attributed to the formation of lines in a rapidly expanding atmosphere. This is best illustrated by N IV RVs of WN 6–9 stars in the Large Magellanic Cloud (Moffat 1989). Nine stars show N IV RVs that are on average $50 \pm 11(\sigma = 34)$ km s^{-1} more negative than the mean LMC RV, although the He II 4686 Å line shows negligible deviation from the LMC, on average, for 14 stars [ΔRV $= 4 \pm 16(\sigma = 58)$ km s^{-1}].

The strongest argument in favour of the W-R + c nature of HD 197406 emerging from our data is the observed phase delay (toward $\phi \sim 0.7$–0.8 instead of $\phi \sim 0.5^{+0.2}_{-0.3}$ expected for a "normal" companion) for the reaction of He I lines on the presence of the ionizing companion.

4. CONCLUSION

Although there is no doubt about the binary nature of HD 197406, we still cannot unambiguously distinguish between the two possibilities for the companion: a normal B-type star or a relativistic object. Note that the low observed X-ray flux is not necessarily an argument against the possibility of an accreting relativistic companion. A large part of the X-ray power could be channeled elsewhere (e.g., Kulkarni & Narayan 1988). Two ways to clarify the nature of the companion in HD 197406 might be through (*a*) high-resolution observations of the weak absorption lines superposed on the tops of the He II+H and He I emissions, in an attempt to detect their true, complete orbital motion (if any) and resolve their profiles; or (*b*) X-ray monitoring to reveal any orbital X-ray flux modulation. In the case of a W-R + c binary, one expects to see an increase of the X-ray flux around phases $\phi \sim 0.7$–0.8 (from a wake in the W-R wind behind the orbiting companion). If the companion is a normal B2–B4 V–III star, the X-ray flux will be directed more toward the W-R star and hence should be less phase dependent, being intercepted by the dense W-R wind.

Even in the case of a normal V–III companion, the location of the system at least 50 pc above the Galactic plane and the expected, extremely low mass ratio make this system unique among the Population I W-R stars.

S. V. M., A. F. J. M., and R. L. acknowledge monetary aid from NSERC of Canada and FCAR (Québec). S. V. M. is grateful to the Instituto de Astronomía (México) for partial financial support during his visit to San Pedro Martir Observatory. We thank Peter Conti, Marten van Kerkwijk, Roberto Mendez, and Pat Morris for useful discussions. We are grateful to A. Grandchamps and Y. Hervieux for their help in obtaining some of the spectra of HD 197406.

REFERENCES

Andersen, J. 1991, A&A Rev., 3, 91
Antokhin, I. I. 1984, Astron. Tsirk. 1350, 1
Antokhin, I. I., & Cherepashchuk, A. M. 1989, Sov. Astron. Lett., 15(4), 303
Bertiau, F. C., S. J., & Grobben, J. 1969, Ric. Astron., 8, 1
Blake, C. C., Marlborough, J. M., Walker, G. A. H., & Falhman, G. G. 1995, AJ, 109, 2698
Blondin, J. M. 1994, ApJ, 435, 756
Bracher, K. 1979, PASP, 91, 827
Brown, J. C., McLean, I. S., & Emslie, A. G. 1978, A&A, 68, 415
Cherepashchuk, A. M., & Aslanov, A. A. 1984, Ap&SS, 102, 97
Conti, P. S. 1995, private communication
Conti, P. S., Leep, M. E., & Perry, D. N. 1983, ApJ, 268, 228
Drissen, L., Lamontagne, R., Moffat, A. F. J., Bastien, P., & Seguin, M. 1986, ApJ, 304, 188
Dubner, G. M., Niemela, V. S., & Purton, C. R. 1990, AJ, 99, 857
Grigsby, J. A., & Morrison, N. D. 1995, ApJ, 442, 794
Hillier, D. J. 1989, ApJ, 327, 822
Khalack, V. R., & Zhilyaev, B. E. 1995, Kinemat. Phys. Celest. Bodies 13, No. 2, in press
Koenigsberger, G. 1995, in IAU Symp. 163, Wolf-Rayet Stars: Binaries, Colliding Winds, Evolution, ed. K. A. van der Hucht & P. M. Williams (Dordrecht: Kluwer), 538
Kulkarni, S. K., & Narayan, R. 1988, ApJ, 335, 755
Lamontagne, R., Moffat, A. F. J., Drissen, L., Robert, C., & Matthews, J. M. 1995, AJ, submitted
Leitherer, C., Chapman, J. M., & Koribalski, B. 1995, ApJ, 450, 289
Marchenko, S. V., Moffat, A. F. J., Eenens, P. R. J., Hill, G. M., & Grandchamps, A. 1995, ApJ, 450, 811
Miller, G. J., & Chu, Y.-H. 1993, ApJS, 85, 137
Millward, C. G., & Walker, G. A. H. 1985, ApJS, 57, 63
Moffat, A. F. J. 1983, in Proc. Workshop on Wolf-Rayet Stars: Progenitors of Supernovae? ed. M. C. Lortet & A. Pitault (Paris: l'Observatoire), III.13
———. 1989, ApJ, 347, 373
Moffat, A. F. J., & Isserstedt, J. 1980, A&A, 85, 201
Moffat, A. F. J., & Seggewiss, W. 1979, A&A, 77, 128
———. 1980, A&A, 86, 87
Moffat, A. F. J., & Shara, M. M. 1986, AJ, 92, 952
Moffat, A. F. J., et al. 1995, in preparation
Nichols, J. S., & Fesen, R. A. 1994, A&A, 291, 283
Payne-Gaposchkin, C. 1957, The Galactic Novae (Amsterdam: North-Holland)
Peña, M., Peimbert, M., Torres-Peimbert, S., Ruiz, M. T., & Maza, J. 1995, ApJ, 441, 343

Pollock, A. M. T., Haberl, F., & Corcoran, M. F. 1995, in IAU Symp. 163, Wolf-Rayet Stars: Binaries, Colliding Winds, Evolution, ed. K. A. van der Hucht & P. M. Williams (Dordrecht: Kluwer), 512
Rochowicz, K., & Niedzielski, A. 1995, Acta Astron., 45, 307
Schmutz, W., Hamann, W.-R., & Wessolowski, U. 1989, A&A, 210, 236
Shakura, N., & Sunyaev, R. 1973, in IAU Symp. 55, X- and Gamma-Ray Astronomy, ed. H. Bradt & A. Giacconi (Dordrecht: Reidel), 155
Smith, L. J., & Willis, A. J. 1994, in Instability and Variability of Hot-Star Winds, ed. A. F. J. Moffat, S. Owocki, A. Fullerton, & N. St-Louis (Dordrecht: Kluwer), 189
Stevens, I. R., & Willis, A. J. 1988, MNRAS, 234, 783
St-Louis, N. 1994, in Proc. Workshop on Instability and Variability of Hot-Star Winds, ed. A. F. J. Moffat, S. Owocki, A. Fullerton, & N. St-Louis (Dordrecht: Kluwer), 197
St-Louis, N., Moffat, A. F. J., Drissen, L., Bastien, P., & Robert, C. 1988, ApJ, 330, 286
Tylenda, R., Acker, A., & Stenholm, B. 1993, A&AS, 102, 595
Underhill, A. B., & Yang, S. 1991, ApJ, 368, 588
van der Hucht, K. A., Hidayat, B., Admiranto, A. G., Supelli, K. R., & Doom, C. 1988, A&A, 199, 217
van Kerkwijk, M. H., et al. 1992, Nature Phys. Sci., 355, 703
Wilson, O. C. 1948, PASP, 60, 385
Zhilyaev, B. E., Khalack, V. R., & Verlyuk, I. A. 1995, in IAU Symp. 163, Wolf-Rayet Stars: Binaries, Colliding Winds, Evolution, ed. K. A. van der Hucht & P. M. Williams (Dordrecht: Kluwer), 550